Coarsening of polyhedral grains in a liquid matrix

Yang-Il Jung
Center for NanoInterface Technology, Department of Materials Science and Engineering, Korea Advanced Institute of Science and Technology, Daejeon 305-701, Republic of Korea

Duk Yong Yoon
Center for NanoInterface Technology, Department of Materials Science and Engineering, Korea Advanced Institute of Science and Technology, Daejeon 305-701, Republic of Korea; and Korea Research Institute of Standards and Science, Daejeon 305-340, and Pohang University of Science and Technology, Pohang 790-784, Republic of Korea

Suk-Joong L. Kang[a)]
Center for NanoInterface Technology, Department of Materials Science and Engineering, Korea Advanced Institute of Science and Technology, Daejeon 305-701, Republic of Korea

(Received 13 January 2009; accepted 20 April 2009)

The coarsening of polyhedral grains in a liquid matrix was calculated using crystal growth and dissolution equations used in crystal growth theories for faceted crystals. The coarsening behavior was principally governed by the relative value of the maximum driving force for growth (Δg_{max}), which is determined by the average size and size distribution, to the critical driving force for appreciable growth (Δg_c). When Δg_{max} was much larger than Δg_c, pseudonormal grain coarsening occurred. With a reduction of Δg_{max} relative to Δg_c, abnormal grain coarsening (AGC, when $\Delta g_{max} \geq \Delta g_c$) and stagnant grain coarsening (SGC, when $\Delta g_{max} < \Delta g_c$) were predicted. The observed cyclic AGC and incubation for AGC in real systems with faceted grains were explained in terms of the relative value between Δg_{max} and Δg_c. The effects of various processing and physical parameters, such as the initial grain size and distribution, the liquid volume fraction, step free energy, and temperature, were also evaluated. The calculated results were in good agreement with previous experimental observations.

I. INTRODUCTION

Grain coarsening in a liquid matrix (Ostwald ripening) is commonly categorized into two types: normal grain coarsening (NGC) and abnormal grain coarsening (AGC). When NGC occurs, the microstructure changes in a uniform manner such that a relatively narrow size distribution of grains results, and the normalized grain size distribution is independent of time and, hence, scale. In contrast, AGC is characterized by the rapid growth of a small number of grains with the consumption of small matrix grains, and hence often features the development of a bimodal grain size distribution. With further annealing, however, the large abnormal grains impinge upon each other, and the grain-size distribution reverts to a unimodal distribution.

In many investigations,[1–17] it has been observed that the mode of grain coarsening is closely related to interface morphology. Normal grain coarsening was observed for macroscopically rounded (atomically disordered and rough) interfaces and abnormal grain coarsening or coarsening inhibition for macroscopically flat (atomically ordered and faceted) interfaces. The normal grain coarsening behavior for rough interfaces has been explained in terms of diffusion-controlled growth, as rough interfaces provide an unlimited number of sites for growth.[18,19] Lifshitz and Slyozov[20] and Wagner[21] considered diffusion-controlled grain coarsening for a system where there is no overlap of diffusional fields among grains (in fact, an infinitely dispersed system) (Lifshitz–Slyozov–Wagner theory). Later, the LSW theory was modified by a number of researchers to consider the effect of solid volume fraction.[22–27] All of the previous works reported the continuous growth of grains, with a rate linearly proportional to the driving force, and with a nonvarying relative size distribution (stationary size distribution). The only difference among these studies was the absolute rate of growth with respect to the solid volume fraction.[26] Conversely, AGC has been explained in terms of a nonlinear migration of faceted interfaces with driving force, as in the case of the growth of faceted crystals from a solution or vapor.[18,28] For an appreciable migration of a faceted interface, an energetically stable nucleus should form on a flat

[a)]Address all correspondence to this author.
e-mail: sjkang@kaist.ac.kr
This author was an editor of this journal during the review and decision stage. For the *JMR* policy on review and publication of manuscripts authored by editors, please refer to http://www.mrs.org/jmr_policy
DOI: 10.1557/JMR.2009.0356

interface.[1,2,18,19] Growth of faceted grains proceeds with atom attachment on the steps formed along the circumference of the nucleus (the step-growth mechanism or the two-dimensional nucleation mechanism)[1,2,19,29,30] if the grain surfaces are free of defects. Operation of this mechanism with a nonlinear relationship between the migration velocity and the driving force can result in AGC when the driving force for growth of only a limited number of grains exceeds the driving force for the formation of atomic nucleation steps.

While the kinetics and behavior for normal coarsening of grains with rough interfaces are well established,[20–23] those for the coarsening of grains with faceted interfaces are not as well understood. Due to the nonlinear relationship between the growth rate and the driving forces for growth, it is difficult to predict the coarsening behavior of faceted grains; the growth rate of a faceted grain can vary with such factors as change of system temperature, the step free energy, and the liquid volume fraction. For this reason, model calculations and simulations have been introduced to understand and predict the coarsening behavior of faceted grains, albeit in a limited number of works, by Wynblatt and Gjostein,[31] Rohrer et al.,[32] and Kang et al.[33] (Since the early 1980s, there have been many simulations on AGC; however, most did not take into account the fact that the coarsening kinetics are strongly dependent on the interface morphology, i.e., rough and faceted.)

Using growth kinetics for a continuous growth mechanism (diffusion control) and a two-dimensional nucleation (2-DN) mechanism (interface reaction control), normal and abnormal grain coarsening, respectively, were described by Wynblatt and Gjostein.[31] They assumed that the effective growth rate is governed either by the diffusion process or the interface reaction process (2-DN) for a faceted grain. For dissolution, the diffusion of atoms was regarded as the sole rate determining process, as atomic dissolution can occur readily at the edge and/or corner of a faceted grain.[19] Wynblatt and Gjostein demonstrated AGC along with NGC using the evolution of the size distribution function, indicating that the two types of grain coarsening behavior are related to the growth mechanism.

Rohrer et al.[32] calculated grain coarsening under the consideration that the growth kinetics is nonlinear for faceted grains, as did Wynblatt and Gjostein. However, as they adopted nonlinear kinetics (2-DN mechanism) for dissolving grains as well as growing grains,[32,34] AGC was not observed in their calculations. Rohrer et al. also calculated the growth of defect-bearing faceted crystals, and predicted NGC, as in the case of rounded grains. They suggested that abnormal grain coarsening is possible only when the dislocations distribute heterogeneously among grains, as grains with defects form abnormal grains and those without defects become matrix grains.[32]

Kang et al.[33] predicted AGC in a system with two-dimensional faceted grains by introducing a numerical solution for a 2-DN mechanism, as previously done by Wynblatt and Gjostein.[31] The results of Kang et al. would be appropriate for explaining AGC observed in two-phase systems with faceted grains. However, they considered a system where the solid volume fraction is negligible, as in the LSW theory. In real systems, where the growth of grains is governed by the slower process between diffusion and interface reaction (mixed control),[35] the liquid volume fraction can also be an important parameter for grain coarsening behavior. The other critical parameters that were not closely examined in the work of Kang et al. are the step free energy (also known as the edge free energy) and the initial grain size.

In the present investigation, model calculations for the coarsening of three-dimensional faceted grains in a liquid matrix were made using the proposed growth kinetics of rounded and faceted grains,[30,31] following the scheme presented in our previous work.[36] Various types of coarsening behavior were obtained, depending on the relative contribution between the maximum driving force ($\Delta g_{\max}$) for grain coarsening and the critical driving force for appreciable growth (Δg_c). Effects of various processing and physical parameters, including the liquid volume fraction as well as the temperature, step free energy, grain size, and initial size distribution, were considered. Successive AGC as well as an incubation time for AGC were predicted for faceted systems, in agreement with the observed AGC behavior.[12,15] General principles of microstructure development in faceted systems have also been suggested.

II. CALCULATION MODEL AND METHOD

The driving force for grain coarsening arises from the difference in sizes among grains, irrespective of their interface structure, and thus the capillary pressure of the grains.[18,19,35] The size of a faceted grain can be defined as given in the Wulff theorem in conjunction with the surface energy. If the growth or dissolution of an individual grain is governed by the interaction with a grain of critical size that is neither growing nor shrinking (the mean field theory assumption), the capillary driving force of a grain of size $2r$, either rounded or faceted, is expressed as

$$\Delta g(r, r^*; t) = 2\gamma V_{\mathrm{m}} \left(\frac{1}{r^*} - \frac{1}{r} \right) \quad . \tag{1}$$

Here, γ is the interfacial energy, V_{m} the molar volume, and $2r^*$ the critical size of grains neither growing nor shrinking, which is the time variant. For spherical grains with a rough interface, the rate of growth is linearly proportional to the driving force.[19–21,35] For angular grains with faceted interfaces, however, grain growth proceeds via step growth mechanisms (2-DN, spiral growth, etc.), where the growth rates are nonlinear functions of the driving force.[18,19,29,30]

When grains are spherical, the growth and dissolution of the grains are controlled by the diffusion of atoms through the matrix. To consider the effect of the matrix volume fraction in the current calculation, the model proposed by Ardell[22] is used. According to Ardell,[22] the rate of continuous grain growth v_D takes the form of

$$v_D \equiv \frac{dr}{dt} = \frac{A}{r}\left(\frac{1}{r^*} - \frac{1}{r}\right)\cdot\left(1 + \beta(\Lambda)\frac{r}{r^*}\right) \quad . \qquad (2)$$

Here, $\beta(\Lambda)$ is a function of the liquid volume fraction (Λ) and $A(= 2\gamma V_m D_f C_\infty/RT$, where D_f is the diffusion coefficient, and C_∞ the concentration of solute far from the interface)[20–22] is a constant depending on the material.

In the case of a faceted grain, attachment of atoms onto a flat surface is usually unstable as a result of the increase in the total interfacial energy accompanied by the attachment, and the attached atoms tend to dissolve again into the liquid matrix. However, once a sufficiently large nucleation island forms, it generates energetically stable ledge and kink sites along the circumference of the nucleus. Therefore, the growth of a faceted grain proceeds with the formation of two-dimensional nuclei, i.e., the 2-DN mechanism,[18,19,29,30,35] if there are no surface atomic steps. The growth rate by 2-DN and growth, v_R, is expressed as

$$v_R \equiv \frac{dr}{dt} = B\exp\left(-\frac{C}{1/r^* - 1/r}\right) \quad . \qquad (3)$$

Here, B and $C(= \pi\sigma^2/6kTh\gamma$, where σ is the step free energy, T the absolute temperature, and h the step height)[19,29] are constants, if polynucleation occurs.[19,29] As the size of growing grains is in the order of microns, the assumption of polynucleation may be acceptable. If intrinsic atomic steps formed by screw dislocations or twins are present on the surface, the growth rate will be higher; however, the growth rate is still expressed as a nonlinear function of the driving force, as in the case of 2-DN.[18,19] In addition, even in the presence of surface defects, screw dislocations or twins, the growth rate can be governed by 2-DN.[37,38] On the other hand, linear kinetics should be applied in the case of dissolution, as each corner acts as a dissolution source without an energy barrier and the dissolution of a grain can occur over multilayers.[18,30,31] As the size of a dissolving grain decreases and approaches the size of a two-dimensional nucleus for growth, there must be an energy barrier for dissolution, as Rohrer et al. noted.[32,34] Nevertheless, as the driving force for dissolution of such an extremely small grain is high, the dissolution of the grain must be governed by diffusion rather than interface reaction. Therefore, the dissolution of a faceted grain must always be governed by diffusion and its kinetics linearly proportional to the driving force for dissolution.

Wynblatt and Gjostein[31] suggested that for the coarsening of faceted noble metal particles in a vapor phase, the rate of coarsening is governed by both 2-DN and vapor transport processes. Given that the time, $1/v$, consumed in forming a complete atom layer on a particle will be the sum of the time for nucleation, $1/v_n$, and the time taken to supply atoms by vapor transport, $1/v_t$, the overall rate of coarsening takes the form of

$$v = \frac{v_n v_t}{v_n + v_t} \quad . \qquad (4)$$

Using a similar concept for the growth of a grain in a liquid matrix, the overall rate of growth can be expressed as

$$\frac{dr}{dt} = \left(\frac{1}{v_D} + \frac{1}{v_R}\right)^{-1} \quad , \qquad (5)$$

for growth by 2-DN.

For calculations, appropriate and realistic values were assumed for physical constants, taking values reported in the literature, including those in Ref. 19 into consideration. The assumed values were $h = 1.2 \times 10^{-10}$m, γ = 0.1 J/m^2, $D_f = 10^{-9}$ m^2/s, C_∞ = 10 at.%, $V_m = 10^{-5}$ m^3, and $\sigma = 0.33h\gamma$ at T = 1773 K. In the case of 2-DN [Eq. (3)], the preexponential value B is known to be in the range of e^{50} to e^{65} m/s.[18] With the assumed values the constant C was calculated to be 2.8×10^7m^{-1}. The constants A and B were then taken to be 1.0×10^{-20}m^3/s and 1.0×10^{25}m/s, as default values.

The starting system consists of one million grains with a Gaussian distribution

$$f(r_0) = \frac{1}{s_0\sqrt{2\pi}}\exp\left[-\frac{1}{2}\left(\frac{r_0 - \bar{r}_0}{s_0}\right)^2\right] \quad , \qquad (6)$$

where $\bar{r}_0$ represents the mean radius and s_0 the standard deviation at time $t = t_0$. To evaluate the rate of growth (or dissolution) of an individual grain, the critical size r^* should be known. This was determined by a binary search, using the mass conservation equation,

$$\sum_{i=1}^{j} r_i^2\left(\frac{\Delta r_i}{\Delta t}\right)_{\text{dissolve}} + \sum_{i=j+1}^{k} r_i^2\left(\frac{\Delta r_i}{\Delta t}\right)_{\text{grow}} = 0 \quad , \qquad (7)$$

where $i = 1, 2, \ldots, k$ indicates the number of grains. The r_i is smaller than r^* for $i < j$, while r_i is larger than r^* for $i \geq j+1$. The mass changes (changes in size) of all of the grains were then calculated using Eqs. (2)–(5). For every calculation time step (CTS), a new r^* is obtained using the same routine, and the incremental/decremental radius of each grain for the next step is determined. For all numeric integrations, the Runge–Kutta method of a fourth order formula was used.

III. RESULTS AND DISCUSSION

Figure 1 is an illustration of the growth and dissolution kinetics given in Eqs. (2) and (3). As shown in Fig. 1, there is a critical driving force Δg_c for appreciable growth

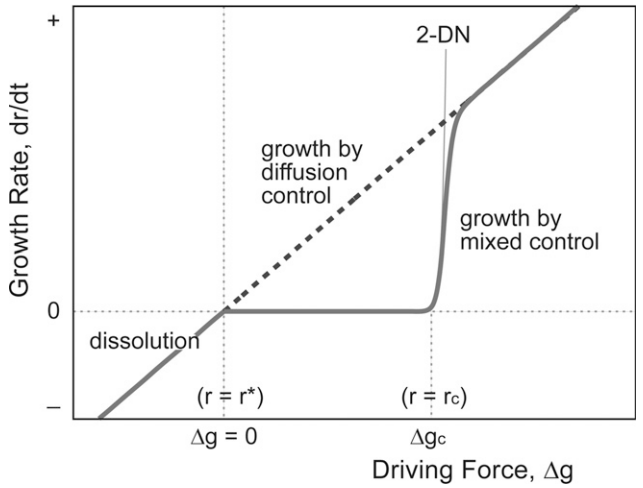

FIG. 1. Schematic showing the variation of growth rate with driving force for two different growth modes: diffusion-controlled growth and mixed-control growth.

in the case of mixed control, in contrast to linear growth in the case of diffusion control. For mixed control, three types of grains are present—the first is growing grains ($r > r_c$) whose growth rate is linearly proportional to the driving force, the second is essentially stagnant grains ($r^* \leq r < r_c$), and the third is dissolving grains ($r < r^*$). In the case of mixed control kinetics, the growth rate is strongly affected by the constants *A*–*C* given in Eqs. (2) and (3), particularly the constant *C*. As the constant *C* affects the growth rate exponentially, it changes the value of the critical driving force Δg_c and drastically alters the growth behavior of grains in a system.

Because there is a nonlinear range in the variation of growth rate with driving force, the relative contribution of this range to the overall coarsening must govern the coarsening behavior of the system. The relative contribution should be governed by the value of the critical driving force Δg_c relative to the (maximum) driving force for growth, which varies with annealing time due to grain coarsening. The relative size distribution should also vary and be nonstationary. In this respect, the grain coarsening behavior can be classified into two types, stationary and nonstationary, unlike the conventional classification of normal and abnormal.

We first examine the relative contribution of the nonlinear range in terms of the effect of the driving force for growth for a given Δg_c followed by the effect of Δg_c for a given driving force. The effect of some specific parameters, including size distribution, liquid volume fraction, and temperature, are subsequently discussed.

A. General behavior

1. Effect of driving force for coarsening

The driving force for coarsening in a system is mostly governed by the average particle size, because the driving force for growth or dissolution of an individual grain is proportional to the difference in curvature between the average size grain and the grain concerned. A change in the average particle size for a given critical driving force results in a change in the relative contribution of the nonlinearity region to the overall coarsening behavior of the system.

Figures 2(a)–2(c) show the calculated change in the grain size distribution with calculation time steps for different initial average sizes of particles at a given step free energy. The results demonstrate the effect of the driving force. In these plots, the frequency distributions of the grains are overlapped on the growth rate curves. The changes in average grain size, $\bar{r}$, the size of the largest grain, r_{max}, and the size of the largest grain (r_{max}) normalized to the average size, $r_{max}/\bar{r}$, with calculation time steps, are also plotted at the end of each series of plots. In the case of $\bar{r}_0 = 0.5$ μm, where $\Delta g_{max} > \Delta g_c$, several rounds of AGC occur, as shown in Fig. 2(a). However, the AGC behavior in Fig. 2(a) is not as distinctive as the conventional AGC, where abnormal grains much larger than the matrix grains appear during annealing. As shown in a plot of the average grain radius with calculation time steps at the end of Fig. 2(a), the change in the average size of grains with calculation time steps is close to that calculated (shown as a dotted curve) for normal coarsening. This apparently pseudo-normal coarsening behavior is due to the considerable number of grains that have driving forces larger than the critical driving force for appreciable growth.

As the initial average size increases, the Δg_{max} decreases, and the number of particles having driving forces larger than Δg_c decreases. When $\Delta g_{max} \approx \Delta g_c$, only a small number of grains initially have driving forces larger than Δg_c, as in the case shown in Fig. 2(b), where $\bar{r}_0 = 1.0$ μm. Only a small number of grains grow abnormally fast with the consumption of all of the other grains. This results in the formation of a small number of large abnormal grains, as shown in the plot in Fig. 2(b) at 200 CTS, which is typical of conventional AGC. When the abnormal grains impinge upon each other, the maximum driving force can become far below Δg_c and it appears that no further grain coarsening can occur for a considerable period of time, as given by the subsequent calculation presented in Fig. 2(b).

When $\Delta g_{max} < \Delta g_c$ [Fig. 2(c)], none of the grains apparently grow and grain coarsening is initially suppressed. Even in this case, however, the grains that are larger than the critical size grain grow slowly with time, following Eq. (3), while the grains that are smaller than the critical size grains dissolve, maintaining the condition of mass conservation. Because the largest grain has the highest growth rate, although it grows slowly, it can reach a driving force larger than Δg_c after a certain period of time. AGC can then suddenly occur after an incubation time.

This incubated AGC, which can often result in distinctive AGC, is shown in Fig. 2(c). If, however, the initial average size is large and Δg_{max} is much smaller than Δg_c, grain coarsening will be suppressed for a considerable period of time, showing stagnant grain coarsening (SGC) behavior.

The predicted change in coarsening behavior with initial particle size has, indeed, been observed in real systems.[2,12,39,40] As the initial size of particles (grains) increased in the WC–Co-based system[2,12,39] and the $BaTiO_3$–TiO_2 system,[40] the growth behavior changed from abnormal to incubated abnormal or stagnant. When the starting powder is of fine size and the annealing time is extremely long, all types of coarsening behavior, from pseudonormal to abnormal and stagnant, may appear successively in the same system. Experimental verification of this, however, has not yet been made.

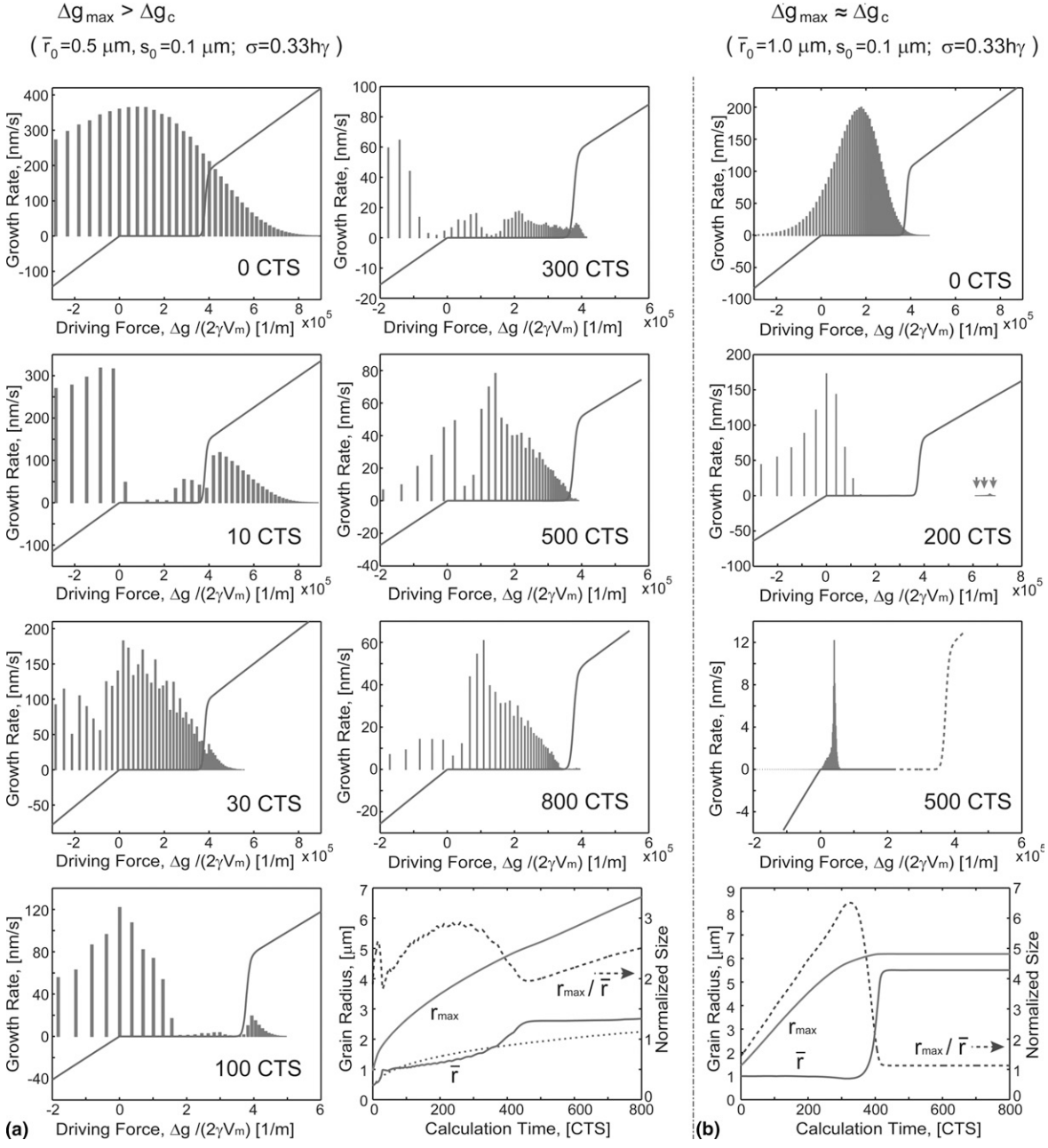

FIG. 2. Calculated evolution of the size distribution with calculation time steps at 1773 K in a system with a step free energy of $\sigma = 0.33h\gamma$ and a liquid volume fraction $\Lambda = 0.15$ for (a) $\bar{r}_0 = 0.5$ μm, $s_0 = 0.1$ μm; (b) $\bar{r}_0 = 1.0$ μm, $s_0 = 0.1$ μm; and (c) $\bar{r}_0 = 1.6$ μm, $s_0 = 0.1$ μm, and that in a system with $\bar{r}_0 = 0.5$ μm, $s_0 = 0.1$ μm for (d) $\sigma = 0.57h\gamma$ and (e) $\sigma = 0.99h\gamma$, respectively. The arrows in the plots indicate abnormal grains. The critical variations in the average grain size and the relative size of the largest grain to the average size grain for each case are also presented at the end of each series of plots. (*continued on next page*)

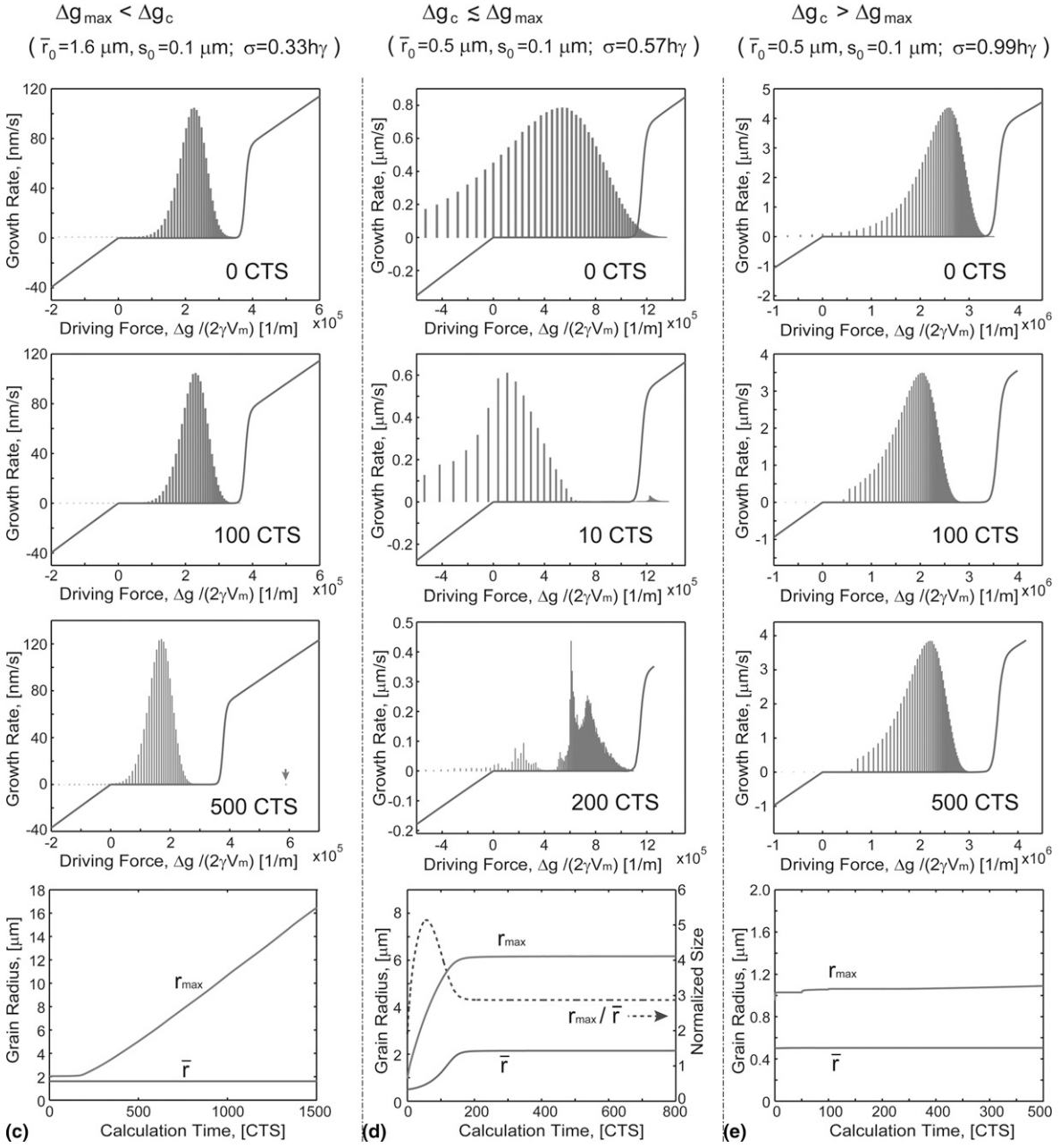

FIG. 2. *(continued)*

2. Effect of critical driving force (Δg_c)

According to crystal growth theories,[18,30] the critical driving force Δg_c can be expressed as

$$\Delta g_c = D\frac{\pi\sigma^2}{kTh} \quad , \tag{8}$$

where D is a constant, which is effectively independent of the step free energy, temperature, and step height. Equation (8) indicates that Δg_c is proportional to the square of σ. A change in σ is achievable by changing the temperature,[11,41–43] adding dopants,[5,6,8,11,41,44–47] or, in the case of oxides, changing the oxygen partial pressure, Po_2.[8,15,40,48] In general, an increase in the total vacancy concentration decreases σ due to the enhanced contribution of mixing entropy.[19]

For a given average size and size distribution in a system, a change in Δg_c results in a change in the relative width of the nonlinearity region, as in the converse case where Δg_c is constant and Δg_{max} is a variable. As Δg_c increases, the contribution of the nonlinearity region increases. This effect is similar to that of an increase in initial particle size, which reduces Δg_{max}, for a system with a constant Δg_c. Therefore, with an increase in the

step free energy from zero to a high value, the coarsening behavior can change from NGC (zero σ) to pseudo-NGC (low σ, where $0 < \Delta g_c << \Delta g_{max}$), AGC (high σ, where $\Delta g_c \leq \Delta g_{max}$), and SGC (very high σ, where $\Delta g_c > \Delta g_{max}$).

Figures 2(a), 2(d), and 2(e) show the calculated variation of the coarsening behavior with changing step free energy. (For the step free energy smaller than $h\gamma$, the grains are partially rounded.[63] Nevertheless, the growth of partially rounded grains is governed by the growth of facets.[10,16]) When the step free energy is zero ($\Delta g_c = 0$), normal grain coarsening occurs, as indicated by a dotted curve in the last plot of Fig. 2(a), following the LSW theory. When the step free energy is low, at $0.33h\gamma$ [Fig. 2(a)], where $\Delta g_c < \Delta g_{max}$, pseudo-NGC (multiple AGC) occurs. As Δg_c increases with an increase in the step free energy, AGC [Fig. 2(d)] and SGC [Fig. 2(e)] occur.

Change in the coarsening behavior from stagnant to abnormal and further to normal was observed in a $BaTiO_3$ system with a reduction of the step free energy by reducing the oxygen partial pressure.[15] A change from AGC to (pseudo-)NGC with a reduction of σ has also been observed for Al_2O_3 with MgO addition,[45,49] NbC–Fe with B addition,[4] α-SiC with atmosphere change,[7] and $SrTiO_3$ with Po_2 reduction or donor-doping.[8]

B. Effects of processing parameters

1. Particle-size distribution

As the number of grains with driving forces larger than Δg_c varies with the size distribution as well as the average size, the size distribution must also considerably affect the coarsening behavior. Figure 3(b) plots the variation of average grain radius and maximum grain radius normalized to the average grain radius for the system shown in Fig. 3(a), where the average sizes are the same but the size distributions are different. In this system, the number of grains that have driving forces larger than Δg_c increases with the broadening of the size distribution. The coarsening behavior thus changes from AGC to pseudo-NGC with the distribution broadening.

When a large grain is present in a fine grain matrix, the grain has a size advantage for rapid growth. It was, however, reported that in the case of solid-state grain coarsening with the mean field theory assumption (this is similar to diffusion-controlled coarsening), a large grain of more than twice the average size has a negative relative growth rate value.[50] Furthermore, the relative size of the large grain to the average size grain is reduced and the large grain is included in the distribution of NGC during extended annealing. In the case of mixed control, NGC behavior may no longer be exhibited, as the relative growth rate of a large grain can take a positive value. In real systems, the size distribution of the raw powder often deviates from the normal distribution

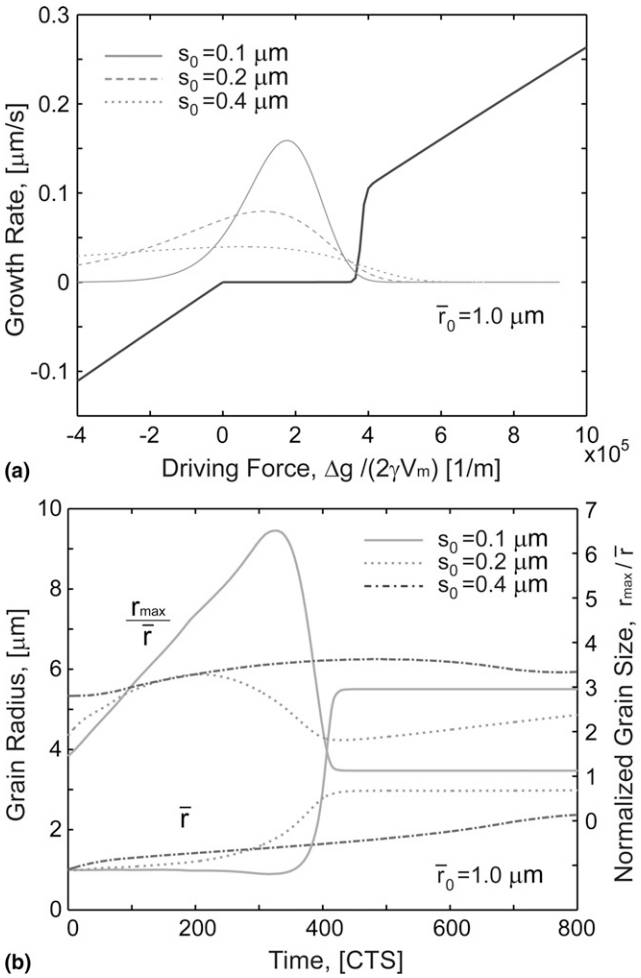

FIG. 3. (a) Growth rate of grains as well as the initial Gaussian distributions of grains in a system with $\bar{r}_0 = 1.0$ μm and $s_0 = 0.1$, 0.2, 0.4 μm as a function of driving force. (b) Variations in average grain size and the ratio of the largest grain size to the average size with calculation time steps for the system shown in (a). System with $\sigma = 0.33h\gamma$ and $\Lambda = 0.15$ at 1773 K.

used in our calculation and usually contains larger particles outside of a unimodal distribution. These particles can become large abnormal grains, much more than several times the average size, during subsequent annealing.

Figure 4 plots the growth curves when a seed crystal of 100 μm radius is inserted in an initial Gaussian distribution of $\bar{r}_0 = 1.0$ μm, $s_0 = 0.1$ μm. The growth behavior of the grains without the seed crystal showed stagnation (SGC) only for the CTS up to 200, as presented in Fig. 2(c). In the presence of the seed crystal, however, SGC is maintained and the seed crystal grows continuously until the complete dissolution of all the grains.

In the solid-state single crystal growth (SSCG) technique,[11,47,51–58] a single crystal seed is usually adjoined to a polycrystal. The growth condition of the seed crystal is largely governed by the average size and size distribution of the matrix grains. To realize the maximum driving

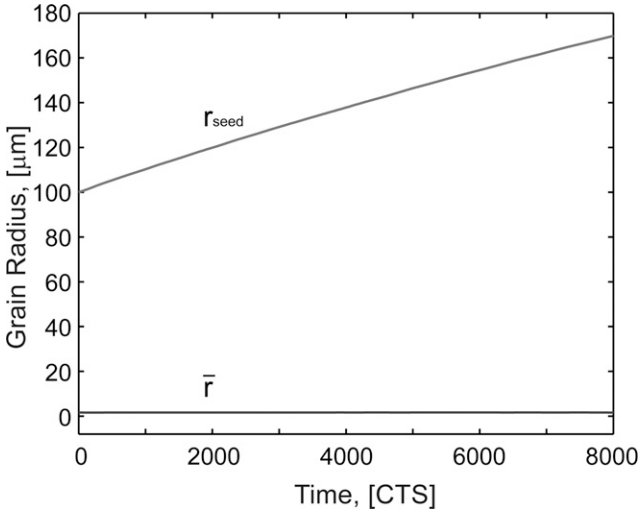

FIG. 4. Increase in the size of a seed crystal ($r_{seed} = 100$ μm at the beginning) with calculation time steps. System with an initial Gaussian distribution of $\bar{r}_0 = 1.6$ and $s_0 = 0.1$ μm, $\Lambda = 0.15$, and $\sigma = 0.33h\gamma$ at 1773 K.

force for single crystal growth, the average size must be as small as possible without rapid growth. The optimal size of the matrix grains for single crystal growth may be predicted by a calculation similar to that given in Fig. 4.

2. Liquid volume fraction

The increase in the liquid volume fraction denotes an increase in the diffusion distance of atoms between grains. Because the growth of the grains is expected to be governed by material transport through the liquid pockets at triple and quadruple junctions, this dependence of diffusion distance on the liquid volume fraction is valid even for systems with grains that are in contact. In the present calculations, however, Ardell's assumption[22] regarding the diffusion geometry was adopted, wherein the particle-to-particle distance is approximately inversely proportional to the liquid volume fraction (particle-to-particle distance $l \approx \bar{r}_0 \frac{e^{8\varphi}\int_{8\varphi}^{\infty} x^{-2/3}e^{-x}dx}{3\varphi^{1/3}}$, where $\varphi = 1 - \Lambda$). Figure 5(a) illustrates the growth rates of grains having an initial Gaussian size distribution with $\bar{r}_0 = 0.5$ and $s_0 = 0.1$ μm for various liquid volume fractions. The growth rate under a driving force larger than the critical value decreases considerably as the liquid volume fraction increases.

Figure 5(b) shows the change in the maximum grain size relative to the average size grain with respect to the liquid volume fraction. With a reduction of the liquid volume fraction, the growth/dissolution rate of individual grains increases and distinctive abnormal grain coarsening results. In systems with a high liquid volume fraction, however, the difference in the growth rate between fast growing grains and stagnant matrix grains is not significant; abnormal coarsening behavior is thereby substantially reduced [Fig. 5(b)]. Such a dependence of

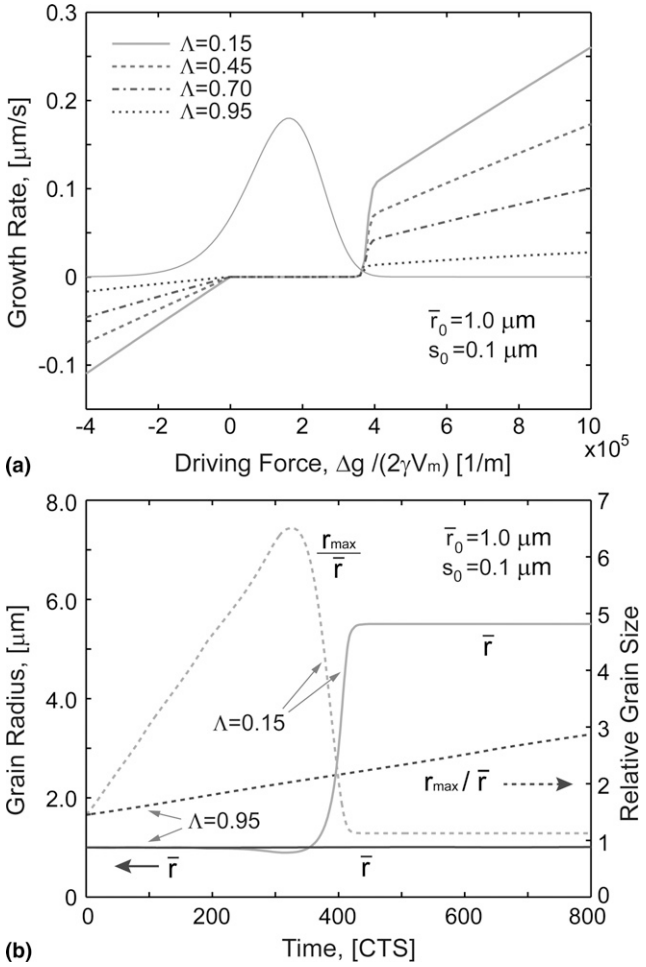

FIG. 5. (a) Growth rates of grains in systems having initial Gaussian size distributions of $\bar{r}_0 = 1.0$ μm, $s_0 = 0.1$ μm for various liquid volume fractions. (b) Variations in average grain size and the ratio of the largest grain size to the average grain size in the system shown in (a) with liquid volume fractions of 0.15 and 0.95.

coarsening behavior on liquid volume fraction was experimentally observed in an Al_2O_3-anorthite,[9] and CaO–Al_2O_3–SiO_2 (CAS) system.[59]

3. Temperature

Two major changes occur in systems when the temperature changes, in relation to the step free energy and the diffusion rate. It is well documented that the step free energy decreases as the temperature increases due to an increased contribution of mixing entropy.[19,60–62] A common expression of the variation in step free energy with temperature takes the form

$$\sigma \approx \sigma_0 \times \exp\left(-\frac{M}{\sqrt{T_R - T}}\right) \quad , \qquad (9)$$

where M is a nonuniversal constant and T_R is the roughening transition temperature.[62] The values of σ_0 and M were taken to be $1.0h\gamma$ and 16.7, respectively, for the calculation, under the assumption of T_R = 2000 K and

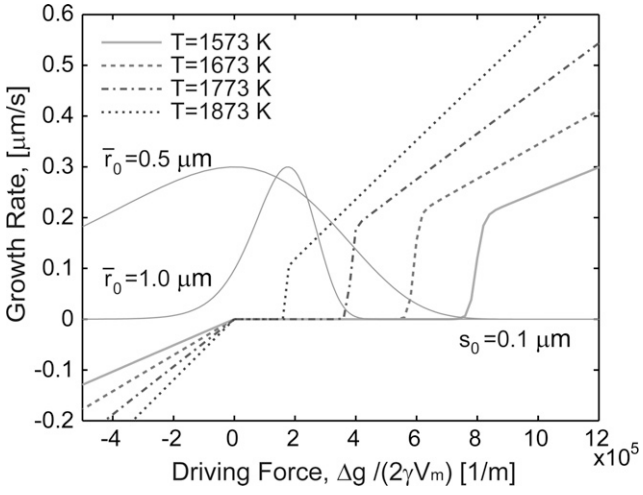

FIG. 6. Growth rates as well as the initial Gaussian distributions of grains at various temperatures in a system with $\bar{r}_0 = 0.5$, 1.0 μm, and $s_0 = 0.1$ μm.

$\sigma = 0.33h\gamma$ at 1773 K. As the temperature and step free energy constitute the term of σ^2/T in the equation of the nucleation rate [C in Eq. (3)], the values of σ^2/T were incorporated into the calculation as parameters for the temperature. For the diffusion rate, the activation energy for an atomic jump Δg_θ was taken to be 10R kJ/mol, a common value for diffusion in liquid.

Figure 6 illustrates growth kinetics with temperature for grains having an initial Gaussian size distribution with $\bar{r}_0 = 0.5$ or 1.0 μm and $s_0 = 0.1$ μm. The size distributions were plotted for T = 1773 K. As the temperature increases, the growth rate increases due to enhanced diffusion, and the number of grains with driving forces larger than Δg_c also increases. Given that a temperature increase decreases σ, and hence Δg_c, the effect of temperature is similar to that of Δg_c if the temperature effect on the diffusion rate is ignored. The coarsening behavior with respect to temperature is thus similar to that with respect to Δg_c; with a temperature increase, the coarsening behavior can change from stagnant to abnormal, pseudonormal, and finally to normal. The observations of an increase in the number of abnormal grains with temperature increase in WC–Co,[2] $BaTiO_3$,[40] and PMN-PT[11] systems reflect that the studied temperature ranges for the systems were for AGC. On the other hand, the change in coarsening behavior from abnormal to normal with increasing temperature in the NbC–Co system[10] indicates that the temperature increase resulted in values of zero for σ and Δg_c, as revealed by a grain shape change from faceted to spherical.

IV. CONCLUDING REMARKS

Model calculations for the coarsening of faceted grains were conducted using available crystal growth and dissolution equations[18,19] of mixed control (diffusion and interface control) and diffusion control for growth and dissolution, respectively. The effects of critical parameters, including the step free energy, the initial particle size and distribution, temperature, and liquid volume fraction, on the coarsening kinetics and behavior were predicted. The coarsening behavior was principally governed by the relative value of the maximum driving force for growth, Δg_{max}, to the critical driving force for appreciable growth, Δg_c. If Δg_c is zero, normal grain coarsening occurs with a stationary size distribution, as predicted by the LSW theory. If Δg_c has a finite value, nonstationary grain coarsening, including pseudonormal, abnormal, and stagnant grain coarsening, occurs.

When the maximum driving force (Δg_{max}) decreases by increasing the initial average particle size for a given Δg_c, pseudo-NGC ($\Delta g_{max} >> \Delta g_c$), AGC ($\Delta g_{max} \geq \Delta g_c$), and SGC ($\Delta g_{max} < \Delta g_c$) can occur consecutively. For $\Delta g_{max} >> \Delta g_c$, however, successive pseudo-NGC followed by AGC and eventually SGC can proceed, if the sample is annealed for an extended period of time. SGC with a unimodal distribution is a result of the completion of the final AGC. Even in the case of highly suppressed GC, however, AGC can occur after an extended annealing time, as the relative growth rate of the largest grain, although not considerable, is the highest, and the largest grain may eventually have a driving force larger than Δg_c. This belated AGC reflects an incubation time for AGC, which has been observed in many systems.

An increase in Δg_c, for a given initial size distribution through an increase in the step free energy or by decreasing the temperature, results in a similar change in the coarsening behavior to that observed on a grain size increase. A temperature change, however, has an additional effect on the diffusion rate. The rate of grain coarsening increases for an identical Δg_c. If the effect of temperature on Δg_c is ignored, the effect of an increase of temperature on the grain coarsening is found to be similar to that of a reduction in the liquid volume fraction, which decreases the diffusion distance and hence increases the coarsening rate. More distinctive AGC occurs with a reduction of the liquid volume fraction.

ACKNOWLEDGMENTS

This work was supported by a grant from the Korea Science and Engineering Foundation, Korea (Grant No. R17-2008-005-01000-0) and by the Korea Research Foundation Grant funded by the Korean Government (MOEHRD)(KRF-2005-005-J09701).

REFERENCES

1. S-J.L. Kang and S-M. Han: Grain-growth in Si_3N_4-based material. *MRS Bull.* **20,** 33 (1995).
2. Y.J. Park, N.M. Hwang, and D.Y. Yoon: Abnormal growth of faceted WC grains in a Co liquid matrix. *Metall. Mater. Trans. A* **27,** 2809 (1996).

3. M.M. Seabaugh, I.H. Kerscht, and G.L. Messing: Texture development by templated grain growth in liquid-phase-sintered α-alumina. *J. Am. Ceram. Soc.* **80,** 1181 (1997).
4. K-S. Oh, J-Y. Jun, D-Y. Kim, and N.M. Hwang: Shape dependence of the coarsening behavior of niobium carbide grains dispersed in a liquid iron matrix. *J. Am. Ceram. Soc.* **83,** 3117 (2000).
5. K. Choi, N.M. Hwang, and D-Y. Kim: Effect of grain shape on abnormal grain growth in liquid-phase-sintered $Nb_{1-x}Ti_xC$–Co alloys. *J. Am. Ceram. Soc.* **85,** 2313 (2002).
6. J.S. Wallace, J.M. Huh, J.E. Blendell, and C.A. Handwerker: Grain growth and twin formation in 0.74PMN–0.26PT. *J. Am. Ceram. Soc.* **85,** 1581 (2002).
7. C-W. Jang, J. Kim, and S-J.L. Kang: Effect of sintering atmosphere on grain shape and grain growth in liquid-phase-sintered silicon carbide. *J. Am. Ceram. Soc.* **85,** 1281 (2002).
8. S-Y. Chung, D.Y. Yoon, and S-J.L. Kang: Effects of donor concentration and oxygen partial pressure on interface morphology and grain growth behavior in $SrTiO_3$. *Acta Mater.* **50,** 3361 (2002).
9. C.W. Park and D.Y. Yoon: Abnormal grain growth in alumina with anorthite liquid and the effect of MgO addition. *J. Am. Ceram. Soc.* **85,** 1585 (2002).
10. Y.K. Cho, D.Y. Yoon, and B-K. Kim: Surface roughening transition and coarsening of NbC grains in liquid cobalt-rich matrix. *J. Am. Ceram. Soc.* **87,** 443 (2004).
11. J.G. Fisher, M-S. Kim, H. Lee, and S-J.L. Kang: Effect of LiO_2 and PbO additions on abnormal grain growth in the $PbMg_{1/3}Nb_{2/3}O_3$–35 mol% $PbTiO_3$ system. *J. Am. Ceram. Soc.* **87,** 937 (2004).
12. B-K. Yoon, B-A. Lee, and S-J.L. Kang: Growth behavior of rounded (Ti,W)C and faceted WC grains in a Co matrix during liquid phase sintering. *Acta Mater.* **53,** 4677 (2005).
13. E.P. Gorzkowski, H.M. Chan, and M.P. Harmer: Effect of PbO on the kinetics of {001} $Pb(Mg_{1/3}Nb_{2/3})O_3$–35 mol% $PbTiO_3$ single crystals grown into fully dense matrices. *J. Am. Ceram. Soc.* **89,** 856 (2006).
14. W. Jo, D-Y. Kim, and N.M. Hwang: Effect of interface structure on the microstructural evolution of ceramics. *J. Am. Ceram. Soc.* **89,** 2369 (2006).
15. J. Chang and S-J.L. Kang: Step free-energy change and microstructural development in $BaTiO_3$–SiO_2. *Key Eng. Mater.* **352,** 25 (2007).
16. K.S. Moon and S-J.L. Kang: Coarsening behavior of round-edged cubic grains in the $Na_{1/2}Bi_{1/2}TiO_3$–$BaTiO_3$ system. *J. Am. Ceram. Soc.* **91,** 3191 (2008).
17. S-J.L. Kang, M-G. Lee, and S-M. An: Microstructural evolution during sintering with control of the interface structure. *J. Am. Ceram. Soc.* **92,** 1464 (2009).
18. J.P. Hirth and G.M. Pound: Condensation and evaporation, nucleation and growth kinetics, in *Progress in Material Science*, Vol. 11, edited by B. Chalmers (Pergamon Press, Oxford, 1963).
19. J.M. Howe: *Interfaces in Materials* (John Wiley & Sons, New York, 1997).
20. I.M. Lifshitz and V.V. Slyozov: The kinetics of precipitation from supersaturated solid solutions. *J. Phys. Chem. Solids* **19,** 35 (1961).
21. C. Wagner: Theory of precipitate change by redissolution (Ostwald ripening). *Z. Elektrochem.* **65,** 581 (1961).
22. A.J. Ardell: The effect of volume fraction on particle coarsening: Theoretical considerations. *Acta Metall.* **20,** 61 (1972).
23. A.D. Brailsford and P. Wynblatt: The dependence of Ostwald ripening kinetics on particle volume fraction. *Acta Metall.* **27,** 489 (1979).
24. P.W. Voorhees and M.E. Glicksman: Ostwald ripening during liquid phase sintering—Effect of volume fraction on coarsening kinetics. *Metall. Trans. A* **15,** 1081 (1984).
25. S.P. Marsh and M.E. Glicksman: Kinetics of phase coarsening in dense systems. *Acta Mater.* **44,** 3761 (1996).
26. R.M. German and E.A. Olevsky: Modeling grain growth dependence on the liquid content in liquid-phase-sintered materials. *Metall. Mater. Trans. A* **29,** 3057 (1998).
27. V.A. Snyder, J. Alkemper, and P.W. Voorhees: The development of spatial correlations during Ostwald ripening: A test of theory. *Acta Mater.* **48,** 2689 (2000).
28. W.K. Burton, N. Cabrera, and F.C. Frank: The growth of crystals and the equilibrium structure of their surfaces. *Philos. Trans. R. Soc. London, Ser. A* **243,** 299 (1951).
29. S.D. Peteves and R. Abbaschian: Growth kinetics of solid-liquid Ga interfaces: Part II. Theoretical. *Metall. Trans. A* **22,** 1271 (1991).
30. D.Y. Yoon, C.W. Park, and J.B. Koo: The step growth hypothesis for abnormal grain growth, in *Ceramic Interfaces 2*, edited by H-I. Yoo and S-J.L. Kang (Institute of Materials, London, 2001), p. 3.
31. P. Wynblatt and N.A. Gjostein: Particle growth in model supported metal catalysts—I. Theory. *Acta Metall.* **24,** 1165 (1976).
32. G.S. Rohrer, C.L. Rohrer, and W.W. Mullins: Coarsening of faceted crystals. *J. Am. Ceram. Soc.* **85,** 675 (2002).
33. M-K. Kang, D-Y. Kim, and N.M. Hwang: Ostwald ripening kinetics of angular grains dispersed in a liquid phase by two-dimensional nucleation and abnormal grain growth. *J. Eur. Ceram. Soc.* **22,** 603 (2002).
34. G.S. Rohrer, C.L. Rohrer, and W.W. Mullins: Nucleation energy barriers for volume-conserving shape changes of crystals with nonequilibrium morphologies. *J. Am. Ceram. Soc.* **84,** 2099 (2001).
35. S-J.L. Kang: *Sintering: Densification, Grain Growth and Microstructure* (Elsevier, Oxford, 2005).
36. S-J.L. Kang, Y-I. Jung, and K-S. Moon: Principles of microstructural design in two-phase systems. *Mater. Sci. Forum* **827–834,** 558 (2007).
37. P. Bennema and J.P. van der Eerden: Crystal graphs, connected nets, roughening transition and the morphology of crystals, in *Morphology of Crystals*, edited by I. Sunagawa (Terra Scientific Publishing Company, Tokyo, Japan, 1987), p. 1.
38. M-K. Kang, Y-S. Yoo, D-Y. Kim, and N.M. Hwang: Growth of $BaTiO_3$ seed grains by the twin-plane reentrant edge mechanism. *J. Am. Ceram. Soc.* **83,** 385 (2000).
39. M. Schreiner, Th. Schmitt, E. Lassner, and B. Lux: On the origins of discontinuous grain growth during liquid phase sintering of WC–Co cemented carbides. *Powder Metall. Inter.* **16,** 180 (1984).
40. Y-I. Jung, S-Y. Choi, and S-J.L. Kang: Grain-growth behavior during stepwise sintering of barium titanate in hydrogen gas and air. *J. Am. Ceram. Soc.* **86,** 2228 (2003).
41. H. Moon, B-K. Kim, and S-J.L. Kang: Growth mechanism of round-edged NbC grains in Co liquid. *Acta Mater.* **49,** 1293 (2001).
42. H. Gabrisch, L. Kjeldgaard, E. Johnson, and U. Dahmen: Equilibrium shape and interface roughening of small liquid Pb inclusions in solid Al. *Acta Mater.* **49,** 4259 (2001).
43. C. Steimer, M. Giesen, L. Verheij, and H. Ibach: Experimental determination of step energies from island shape fluctuations: A comparison to the equilibrium shape method for Cu(100), Cu (111), and Ag(111). *Phys. Rev. B* **64,** 085416 (2001).
44. Y-W. Kim, M. Mitomo, H. Emoto, and J-G. Lee: Effect of initial α-phase content on microstructure and mechanical properties of sintered silicon carbide. *J. Am. Ceram. Soc.* **81,** 3136 (1998).
45. C.W. Park and D.Y. Yoon: Effects of SiO_2, CaO, and MgO additions on the grain growth of alumina. *J. Am. Ceram. Soc.* **83,** 2605 (2000).
46. C.W. Park, D.Y. Yoon, J.E. Blendell, and C.A. Handwerker: Singular grain boundaries in alumina and their roughening transition. *J. Am. Ceram. Soc.* **86,** 603 (2003).
47. T. Motohashi and T. Kimura: Formation of homo-template grains in $Bi_{0.5}Na_{0.5}TiO_3$ prepared by the reactive-templated grain growth process. *J. Am. Ceram. Soc.* **91,** 3889 (2008).

48. P. Shen, H. Fujii, T. Matsumoto, and K. Nogi: The influence of surface structure on wetting of α-Al_2O_3 by aluminum in a reduced atmosphere. *Acta Mater*. **51,** 4897 (2003).
49. C.A. Bateman, S.J. Bennison, and M.P. Harmer: Mechanism for the role of magnesia in the sintering of alumina containing small amounts of a liquid phase. *J. Am. Ceram. Soc*. **72,** 1241 (1989).
50. C.V. Thompson, H.J. Frost, and F. Spaepen: The relative rates of secondary and normal grain growth. *Acta Metall*. **35,** 887 (1987).
51. Y-S. Yoo, M-K. Kang, J-H. Han, H. Kim, and D-Y. Kim: Fabrication of $BaTiO_3$ single crystals by using the exaggerated grain growth method. *J. Eur. Ceram. Soc*. **17,** 1725 (1997).
52. A. Khan, F.A. Meschke, T. Li, A.M. Scotch, H.M. Chan, and M.P. Harmer: Growth of $Pb(Mg_{1/3}Nb_{2/3})O_3$–35 mol% $PbTiO_3$ single crystals from (111) substrates by seeded polycrystal conversion. *J. Am. Ceram. Soc*. **82,** 2958 (1999).
53. P.W. Rehrig, G.L. Messing, and S. Trolier-McKinstry: Templated grain growth of barium titanate single crystals. *J. Am. Ceram. Soc*. **83,** 2654 (2000).
54. E.M. Sabolsky, G.L. Messing, and S. Trolier-McKinstry: Kinetics of templated grain growth of $0.65Pb(Mg_{1/3}Nb_{2/3})O_3$–$0.35PbTiO_3$. *J. Am. Ceram. Soc*. **84,** 2507 (2001).
55. P.T. King, E.P. Gorzkowski, A.M. Scotch, D.J. Rockosi, H.M. Chan, and M.P. Harmer: Kinetics of {001} $Pb(Mg_{1/3}Nb_{2/3})O_3$–35 mol% $PbTiO_3$ single crystals grown by seeded polycrystal conversion. *J. Am. Ceram. Soc*. **86,** 2182 (2003).
56. S-Y. Choi, D.Y. Yoon, and S-J.L. Kang: Kinetic formation and thickening of intergranular amorphous films at grain boundaries in barium titanate. *Acta Mater*. **52,** 3721 (2004).
57. M-S. Kim, J.G. Fisher, and S-J.L. Kang: Grain growth control and solid-state crystal growth by Li_2O/PbO addition and dislocation introduction in the PMN–35PT system. *J. Am. Ceram. Soc*. **89,** 1237 (2006).
58. B-K. Yoon, S-Y. Choi, T. Yamamoto, Y. Ikuhara, and S-J.L. Kang: Grain boundary mobility and grain growth behavior in polycrystals with faceted wet and dry boundaries. *Acta Mater*. **57,** 2128 (2009).
59. C.P. Chen, H.Z. Yang, J.X. Gao, H.W. Sun, and X. Hu: Densification behavior and microstructural evolution of TiO_2/CAS-incorporated alumina. *Ceram. Int*. **35,** 585 (2009).
60. J.M. Kosterlitz: The critical properties of the two-dimensional *xy* model. *J. Phys. C: Solid State Phys*. **7,** 1046 (1974).
61. H. van Beijeren: Exactly solvable model for the roughening transition of a crystal surface. *Phys. Rev. Lett*. **38,** 993 (1977).
62. H. van Beijeren and I. Nolden: The roughening transition, in *Structure and Dynamics of Surfaces II, Vol 43 of Topics in Current Physics*, edited by W. Schommers and P. von Blanckenhagen (Springer-Verlag, Berlin, 1987), p. 259.
63. M. Wortis: Equilibrium crystal shapes and interfacial phase transitions, in *Chemistry and Physics of Solid Surfaces*, Vol. 7**,** edited by R. Banselow and R.F. Howe (Springer Verlag, Berlin, Germany, 1988), p. 367.